Null screens type Hartmann to test simple lenses

Gabriel Castillo-Santiago, Diana Castán-Ricaño, Alfredo Gozález-Galindo, Maximino Avendaño-Alejo, Rufino Díaz-Uribe

Gabriel Castillo-Santiago, Diana Castán-Ricaño, Alfredo Gozález-Galindo, Maximino Avendaño-Alejo, Rufino Díaz-Uribe, "Null screens type Hartmann to test simple lenses ," Proc. SPIE 9575, Optical Manufacturing and Testing XI, 95751H (27 August 2015); doi: 10.1117/12.2188863

SPIE.

Event: SPIE Optical Engineering + Applications, 2015, San Diego, California, United States

Null screens type Hartmann to test simple lenses

Gabriel Castillo-Santiago[a], Diana Castán-Ricaño[a], Alfredo González-Galindo[a], Maximino Avendaño-Alejo[b], Rufino Díaz-Uribe[b]

[a]Facultad de Ingeniería, División de Estudios de Posgrado, Universidad Nacional Autónoma de México.

[b] Centro de Ciencias Aplicadas y Desarrollo Tecnológico, Universidad Nacional Autónoma de México, Cto. Int. S/N, C. P. 04510, D. F. Méx.

ABSTRACT

In order to evaluate either qualitative or quantitatively the shape of fast plano-convex aspheric lenses, a method to design null screens type Hartmann is proposed. The null screens are formed with non-uniform spots, which allows to have uniform images at detection's plane. The screens are printed on a foil sheet and placed in front of the lens under test, they are illuminated with a collimated monochromatic beam propagating along the optical axis, in such a way that through the process of refraction will form a uniform spot patterns which are recorded at a predefined plane of detection. Finally, processing properly its image recorded we could be able to get a quantitative evaluation of the lens under test. The designs of these null screens are based on the equations of the caustic surface produced by refraction. A preliminary test for a fast plano-convex aspheric lens with $F/\# = 0.8$ is presented in this work. This method could also be applied to alignment of optical systems.

1. INTRODUCTION

Nowadays aspheric lenses are widely used in both imaging and no-imaging optical systems, because this kind of lenses eliminate spherical aberration and reduce other aberrations more efficiently than spherical lenses. Among their properties we can state that the radius of curvature changes along the distance with the optical axis. In other words aspheric lenses can help to simplify optical system design by minimizing the number of elements required, additionally, these can yields sharper images than conventional lenses, they are currently useful for correcting distortion in wide angle lenses. To sum up, aspheric lenses deliver higher performing, more compact, and lighter systems in a wide range of applications such as light concentrators, telescopes, intra ocular lenses, or collimators of light.

The traditional Hartmann test uses a screen having a rectangular array of holes with a uniform separation between them, which are based on the spot diagrams obtained through an exact ray tracing, in such a way that the screen is placed close to the entrance or exit pupil of the system under test. The Ronchi test use a ruling with a uniform distribution of fringes alternates between dark and bright strips well defined, which produces either by reflection or refraction a non-uniform distribution of alternate dark and bright fringes at the detection plane only if the optical system have imperfections on the optical surface.[1]The Hartmann and Ronchi tests have been successfully implemented to evaluate either qualitative or quantitatively lenses and mirrors assuming $F/\# > 1$.[2,3] For fast optical surfaces F/#<1, the no-uniformity in the size for each bright spots on the pattern recorded at detection's plane is very common, complicating subsequents analysis in order to evaluate the surface under test, to overcome this problem a null test has been developed for aspherical convex surfaces, in which instead of using an array of point light sources, the null screens are printed by using a common laser printer as was explained in reference.[4]

In earlier papers, special rulings with curved lines were constructed to test spherical concave mirrors and this approach was denominated null Ronchi test. In reference[5] the ruling was computed according to the following procedure: using a ray tracing program, a transverse aberration curve (TA) is computed at an approximate plane

Further author information: Send correspondence to E-mail: maximino.avendano@ccadet.unam.mx, Telephone: 5556228620, Address: Circuito Interior S/N, Ciudad Universitaria, Apdo. Postal 70-186, C. P. 04510, D. F., Méx.

Optical Manufacturing and Testing XI, edited by Oliver W. Fähnle, Ray Williamson, Dae Wook Kim, Proc. of SPIE Vol. 9575, 95751H · © 2015 SPIE · CCC code: 0277-786X/15/$18 · doi: 10.1117/12.2188863

where the ruling will be placed. A system of five linear simultaneous equations is solved in order to determine the coefficients of the aberration polynomial to get a formula for TA. Finally, using geometrical considerations and the computed TA the null screens are designed. Alternatively, in reference[6] a predetermined equation is used to provide TA and with the aid of an expression to compensate the error introduced by the Ronchigram fringes on the mirror surface under test, and assuming some geometrical considerations, an equation was provided an it can be solved numerically by using Newton's method, in order to design null screens.

Recently an alternative method to design null screens in order to test qualitatively a plano-convex spherical lens[7] and roughly quantitatively a plano-convex parabolic lens[8,9] has been proposed, but instead of an array of point light sources, the null screen was printed on an acetate foil using a traditional laser printer specified at 1200 dpi. In this work we extend these ideas to design null screens in order to test aspherical lenses. The null screen will be formed with a no-uniform array of drop spots, in such a way that through the process of refraction we obtain a uniform distribution of circular bright spots with similar sizes at the detection plane, only if the lens under test do not present deformations on its surface. The design of these screens are based on the knowledge of the caustic surface by refraction also called diacaustic or alternatively by using the exact ray tracing through aspherical lenses, considering a plane wavefront propagating along the optical axis impinging on the lens under test.[8] This kind of null screens allows to make straightforward the detection of the spots for the measurement either Longitudinal Spherical Aberration (LSA) or Transversal Spherical Aberration (TSA). The main idea in this work is to retrieve the shape of the lens under test by using null screens through the traditional procedure of either Ronchi or Hartmann tests.

2. THEORY

Throughout this manuscript we define the $\mathbf{Z}$ axis parallel to the optical axis, we assume that the $\mathbf{Y}-\mathbf{Z}$ plane is the plane of incidence, which is a cross section of a plano-convex aspheric lens whose paraxial radius is R, and the origin of the system $\mathcal{O}$ is placed at the first vertex of the lens. We assume that there is rotational symmetry about $\mathbf{Z}$ axis and a bundle of rays are incident on the left side of the lens parallel to the optical axis, crossing the plane face of the lens without being deflected, and they are propagated to the aspheric surface where they are refracted outside of the lens. Let H be the entrance aperture, t the thickness of the lens, n_i the index of refraction of the lens for a predefined wavelength, considering that the lens is immersed in a medium with index of refraction n_a, $(n_i > n_a)$, and where we have assumed that S_{h_N} represents the aspheric equation in a meridional plane which can be written as

$$S_{h_N} = \frac{ch^2}{1+\sqrt{1-(k+1)c^2h^2}} + \sum_{i=1}^{N} A_{2i}\, h^{2i}, \tag{1}$$

where $c = 1/R$ is the paraxial curvature, k is the conic constant, A_2, A_4, $\ldots$, A_{2N}, are the aspheric coefficients with N the number of aspheric terms included in the polynomial and h represents the height for each one of the arbitrary incident rays, where Eq.(1) is valid in the range $h \in [-H, H]$. It is important to state that if $N = 0$, then Eq.(1) is reduced to the equation which represent the profile for conic surfaces. According to reference[8] the caustic surface (z_c, y_c) for a Plano-Convex aspheric lens when the point source is placed at infinity can be written as

$$\begin{aligned} z_c(h) &= t + S_{h_N} + \frac{\left[n_a^2 + (n_a^2 - n_i^2){S'}^2_{h_N}\right]\left[n_a^2 + n_i\sqrt{n_a^2 + (n_a^2 - n_i^2){S'}^2_{h_N}}\right]}{n_a^2(n_a^2 - n_i^2)S''_{h_N}}, \\ y_c(h) &= h - \frac{\left[n_a^2 + (n_a^2 - n_i^2){S'}^2_{h_N}\right] S'_{h_N}}{n_a^2 S''_{h_N}}, \end{aligned} \tag{2}$$

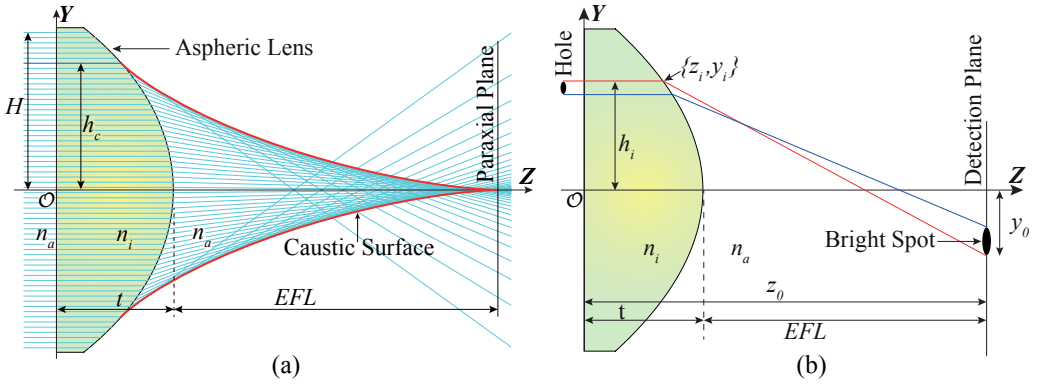

Figure 1. (a) Ray tracing process. (b) Process to design null screens.

where the subscript c means caustic surface and S'_{h_N}, S''_{h_N} are the first and second derivative with respect to h respectively, thus from Eq.(1) we obtain

$$S'_{h_N} = \frac{ch}{\sqrt{1-(k+1)c^2h^2}} + \sum_{i=1}^{N} 2i\, A_{2i}\, h^{2i-1},$$
$$S''_{h_N} = \frac{c}{[1-(k+1)c^2h^2]^{3/2}} + \sum_{i=1}^{N} 2i(2i-1)\, A_{2i}\, h^{2(i-1)}. \tag{3}$$

It is important to remark that Eq.(2) gives the coordinates of the locus of points that parametrically represents the envelope of the family of refracted rays produced by an aspheric lens in a meridional plane as shown in Fig.1(a). From Eq.(2) if the radical $\left[n_a^2 + (n_a^2 - n_i^2)S'^2_{h_N}\right] \leq 0$, then physically there are rays that undergo total internal reflection, where h_c means the critical height, in other words, the incident rays above this value undergo total internal reflection as is shown in Fig.1(a).[8]

3. DESIGN OF RULING FOR THE NULL SCREEN

To design null screens, we can follow all the steps well explained in references,[7,11] where have been used the caustic equation providing a polynomial equation which can be solved through numerical methods, yielding a non-uniform drops which allows to recover a uniform array of spots with similar sizes recorded at a plane of detection only if the surface under test does not have any deformation on their surface. It worth to state that we defined previously the position for the plane of detection, which can be placed at arbitrary distances along the optical axis and being perpendicular to it. Furthermore, it is important to consider the size of the CCD sensor where is recorded the Hartmanngram, taking into account the number of spots already defined to be registered on the active area of the CCD sensor. An alternative method to design null screens is explained as follows: We proceed starting at the detection's plane: The z_i and y_i coordinates of the point of incidence of the ray on the aspheric surface lens are not selected a priori but must be calculated as is traditionally done: given an arbitrary point $P_0 = (z_0, y_0)$ at the detection plane, we trace a ray back through $P_i = (z_i, y_i)$ as is shown in Fig.1(b), by using the exact ray tracing equation through aspheric lens, which according to reference[8] was written as

$$y_0 = \frac{[n_a^2 - n_i^2]\,[z_0 - (t + S_{h_N})]\,S'_{h_N}}{n_a^2 + n_i^2\sqrt{n_a^2 + (n_a^2 - n_i^2)S'^2_{h_N}}} + h, \tag{4}$$

where n_a and n_i are the indexes of refraction, t is the thickness of the lens, y_0 is the height for a point lying on the border of an arbitrary spot, and z_0 is the distance between the vertex of the lens under test and the plane of detection, S_{h_N} and S'_{h_N} are given by Eqs.(1) and (3) respectively. In resume, we can solve numerically Eq.(4) for h providing the values for h_i which will form the null screen as is shown in Fig.1(b). We can notice

that there are two important cases for the positioning of z_0: For $z_0 \geq EFL$, we have a unique solution whose values lie in the range $[0, H]$ for $y_0 < 0$, where H is the entrance aperture of the lens. For $z_0 < EFL$ the plane of detection lies inside the caustic surface. In this particular case there are three possible solutions because we have rays from the lower part and rays arriving from the upper part of the lens which coincide in y_0 when the plane of detection is placed inside of the caustic region, as was explained in reference.[7]

It is important to say that commonly the CCD sensors have a rectangular area with $L_M \times l_m$, where L_M and l_m are the largest and shortest sides of the sensor respectively. To design the null screens in such a way that its image formed by refraction through the lens under test yields a uniform square array of bright spots equally spaced between them at the image plane, we set a square array of spots inside the detection plane as follows: we define a point (z_0, y_0), where z_0 is the distance along the optical axis where the detection plane is placed. In order to provide a circular spot on the null screen, we define y_0 as a length given by $y_0 = (v_{im}^2 + w_{jm}^2)^{1/2}$, where $v_{im} = i \times r_G$, and $w_{jm} = j \times r_G$ for $i, j = 0, 1, \ldots, G$, where G is the number of circular spots lying inside the sensitive area of the CCD sensor, and m is the number of the discrete points to form each one circular spots, additionally we have defined $r_G = l_m/(4G - 2)$. Even more due to the lens under projects a circular area on the CCD sensor in a similar way like the Circle of Least Confusion, we demand to get a length equal to shortest side of the CCD sensor l_m, where for simplicity we have removed the spots lying outside of this circular area, considering their radius as $l_m/2$ as is shown in Fig.2(a). We can notice that $y_0 \in [-l_m/2, +l_m/2]$, and for an arbitrary point $A_p = (v_{im}, w_{jm})$ it could be represented in polar coordinates as $A_p = [v_{im}^2 + w_{jm}^2]^{1/2}(\cos\theta, \sin\theta) = y_0(\cos\theta, \sin\theta)$, where $\theta = \arctan(w_{jm}/v_{im})$, and substituting the values for z_0 and y_0 into Eq.(4) covering all the points for each one circular spots and solving numerically for h, we obtain the values for h_i lengths placed in a meridional plane, demanding that $h_i \in [-D/2, D/2]$, where D is the diameter of the lens under test. We can multiply those values times the angle θ yielding the null screen according to $NS = h_i(\cos\theta, \sin\theta) = (v'_{im}, w'_{jm})$, where NS means null screen as is shown in Fig.2(b). Finally by joining contiguous points belonging to each spots in order to get a close polynomial curve with $m - 1$ points.

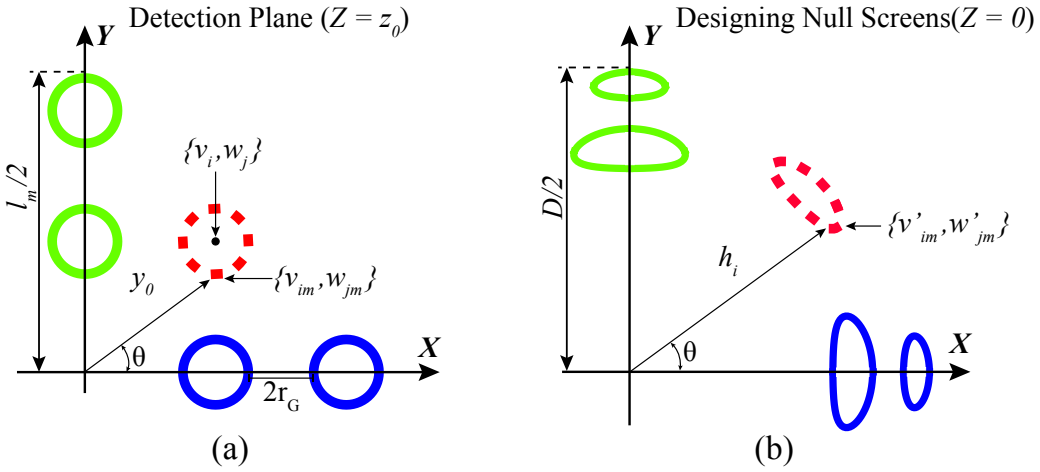

Figure 2. (a) Sample with circular drops in the detection plane. (b) No uniform drops in the incidence plane.

We can extend the ideas explained above to design null screens to test aspheric lenses in the configuration convex-plano, where the exact ray tracing equation assuming a plane wavefront incident on the convex surface according to reference[10] can be written as

$$y_0 = h - \frac{\left[n_i^2 - n_a^2\right]\left[t - S_{h_N}\right]S'_{h_N}}{n_i^2 + n_a\sqrt{n_i^2 + (n_i^2 - n_a^2)S'^2_{h_N}}} - \frac{\left[n_i^2 - n_a^2\right]\left[z_0 - t\right]S'_{h_N}}{\sqrt{n_a^2\left[n_a + \sqrt{n_i^2 + (n_i^2 - n_a^2)S'^2_{h_N}}\right]^2 - [n_i^2 - n_a^2]^2 S'^2_{h_N}}}, \tag{5}$$

by substituting the values for z_0 and y_0, and solving for h from Eq.(5), following all the steps as was explained above we can also obtain the null screens for this configuration. In Fig.(3) are shown three null screens for $G = 7$, 11 and $G = 15$ respectively with $m = 60$ for each spot. We clearly see that increasing the number of bright spots the size of the null screens keep constant for distances z_0 predefined.

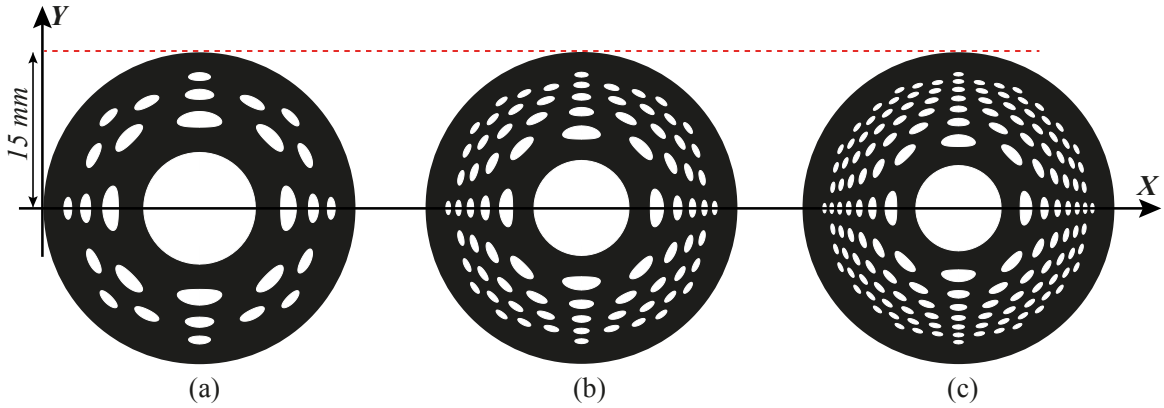

Figure 3. a) $G = 7$ bright spots. b) $G = 11$ bright spots. c) $G = 15$ bright spots, in all the cases $m = 60$, and $z_0 = 1.0EFL$.

4. QUALITATIVE EVALUATION

In this work we evaluate qualitatively a plane-convex aspheric lens. The diagram of the experimental setup is shown in Fig.(4), where we can also see two polarizers which have been used to reduce the intensity of the laser beam incident on the CCD sensor. We have printed the null screens on acetate foils using a 1200 dpi laser printer, assuming a uniform distribution of transparent equally spaced spots at detection plane. The parameters of the aspherical lens are: $R = 13.859$mm, $n_a = 1$ and $n_i = 1.5212$ for $\lambda = 633$nm, diameter $D = 30$mm, effective focal length $EFL = 26.5$mm, with $F/\# = 0.88$, and three aspheric terms $A_2 = 7.9 \times 10^{-6}$, $A_4 = 1.5 \times 10^{-7}$, $A_6 = 1.3 \times 10^{-9}$. We have used a CCD sensor with an active area $A = 6.6$mm$\times 8.8$mm and 480×640pixels respectively. The light source is a He-Ne laser with spatial filtering and a collimated beam, where a collimator lens with $F/\# = 6$ has been implemented to reduce the hot spot by increasing the distance between the collimator lens and the pinhole. The NS have been designed to be placed outside of the caustic surface $z_0 = 1.0EFL$. An important consideration is that if visual observations are made to be in real time, the computed null screen can be calculated to produce an observable pattern of adequate size for the lens under test at a unique detection plane, as is shown Fig.(5) for different images recorded outside of the plane of detection.

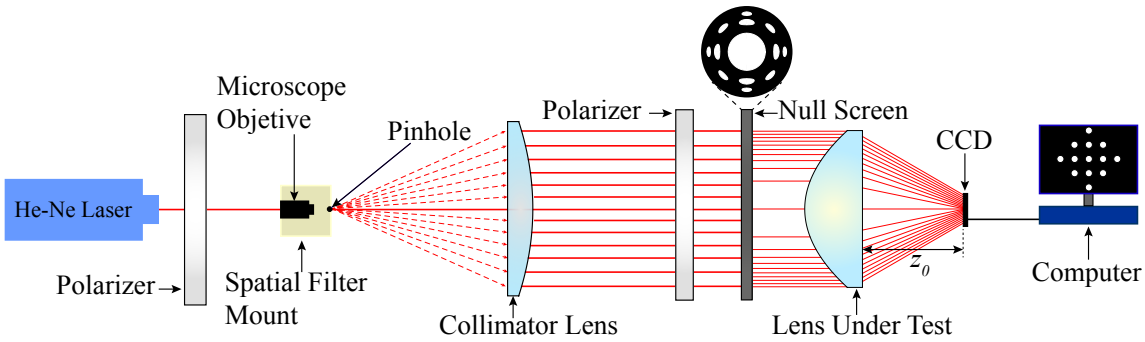

Figure 4. Diagram of the experimental setup to test a plano-convex aspherical lens using null screens.

Following the procedure described above we design null screens as are shown in Fig.6(a) for plano-convex configuration and, Fig.6(c) for convex-plano configuration considering a plane wavefront incident impinging on the

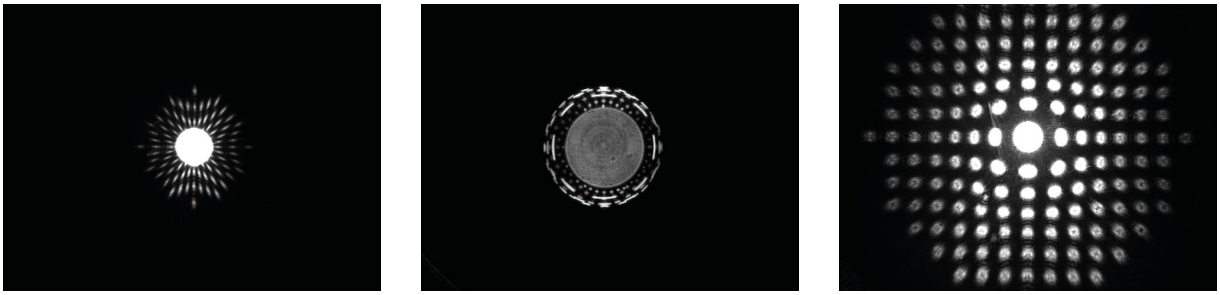

Figure 5. (a) Image recorded inside the caustic region. (b) Image recorded close to circle of least confusion. (c) Image recorded slightly far from plane of detection.

aspheric lens, we predefined 15 bright spots along either **X**-axis or **Y**-axis. As we can notice, the null screen is smaller for plano-convex than convex-plano configuration, due to total internal reflection. Although for the convex-plano configuration there is no total internal reflection, the illuminated area on the lens under test is not covered completely for all the bright spots due to an slight area used by an optical mount on the lens. There is a non-uniformity on the irradiance at the borders of the images recorded on the CCD sensor as are shown in both Fig.6(b) and (d), and they could be produced by several factors, among we can comment: There are losses due to Fresnel's coefficients on transmission through aspheric surface. The shape of the beam laser is Gaussian being more intense at the center than the borders of the beam, although we have used a graduated filter behind of the collimator lens, in order to get a uniform irradiance distribution incident on the CCD sensor, we do not have a uniform bright spots at the plane of detection as we expected.[11]

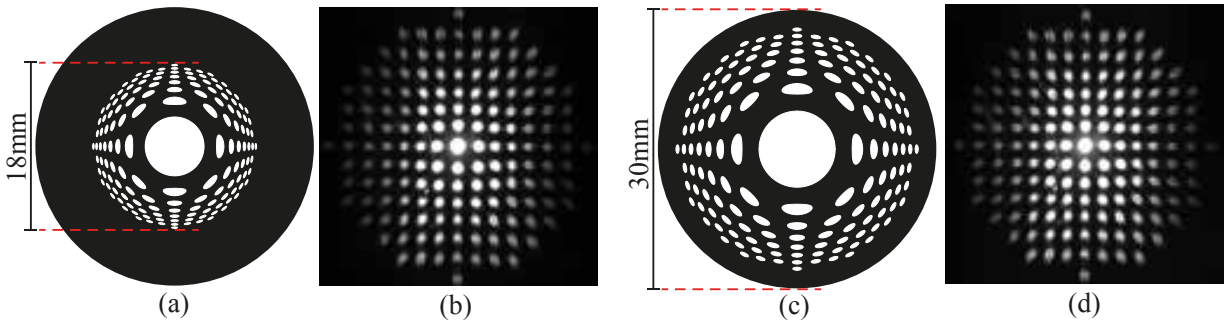

Figure 6. (a) Null screen for a plano-convex aspheric lens. (b) Image recorded at detection's plane for a plano-convex lens. (c) Null screen for a convex-plano lens. (d) Image recorded at detection's plane for a convex-plano lens.

Making a first qualitative analysis of figures 6(b) and (d), we can notice that, in general, the images show an almost regular square grid pattern in the center of the image, except for the borders of the lens where the square grid pattern are slightly curved, and it is easy to determine that in these zones the lens under test departs from the ideal aspheric shape more significantly. Furthermore, some points, near the edge of the lens, look blurred or even more they are vanished. The recorded images deformations are due to the tested surface and not to deformations of the acetate foil where is printed the null screen or even misalignments of the test surface. Then, the null screen method can be used to detect tiny shape deformations of the test surface. The centroids of irradiance of the images recorded are shown in Fig.(7); they were calculated with the image-processing program ImageJ.[12]

Obtaining the experimental centroids from images recorded provided in Fig.6 (b) and (d), and comparing with the ideal centroids which were considered to design the null screens. As was mentioned above, there are some deviations from the expected pattern, due to imperfections on the surface under test. As much as we known from the reference,[13] the transversal aberration for an optical system can be expressed in a polynomial form,

in such a way that the primary aberrations can be analyzed by using the coordinates of the centroids assuming both meridional and sagittal rays, thus, the transversal aberration is written as

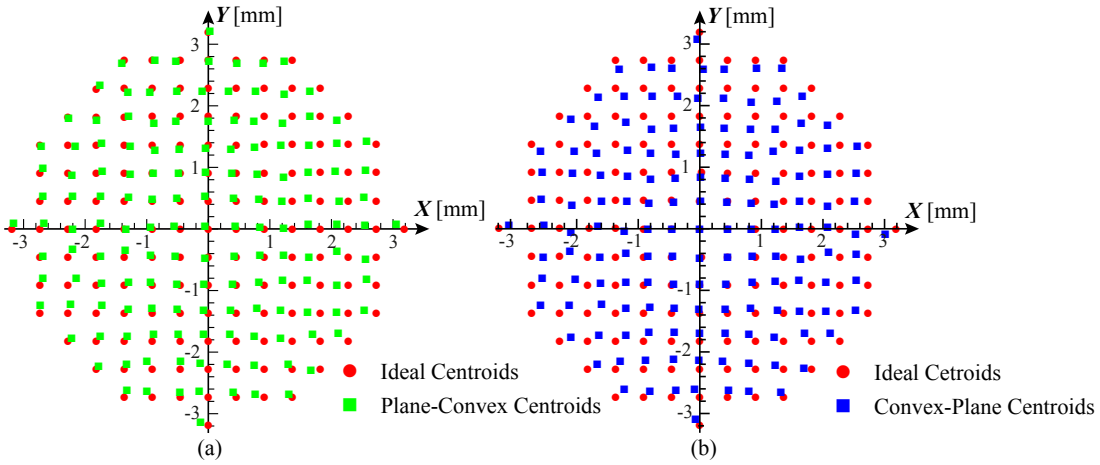

Figure 7. (a) Comparison between ideal and experimental centroids for testing an aspheric lens in plane-convex configuration. (b) Comparison between ideal and experimental centroids for testing a convex-plane aspheric lens.

$$\begin{aligned} TAx(h_x,0) &= -\left[2(D+C)h_x + 4Ah_x^3\right] R \\ &= a_{1xx}h_x + a_{3xx}h_x^3 + A_5, \\ TAy(0,h_y) &= -\left[E + 2(D+3C)h_y + 3Bh_y^2 + 4Ah_y^3\right] R \\ &= a_{0yy} + a_{1yy}h_y + a_{2yy}h_y^2 + a_{3yy}h_y^3 + A_5 \end{aligned} \tag{6}$$

where TAx and TAy are the transverse aberration along the X and Y respectively, h_x and h_y are the components of the beam in the incidence plane, and the constants for primary aberration are given by A= spherical aberration, B = Coma, C = astigmatism, and D = defocus, E = Tilt. Making a bit of algebra we can obtain a relationship between the constants A, B, C, D, E and the primary aberration, finally A_5 represent the fifth spherical aberration order.

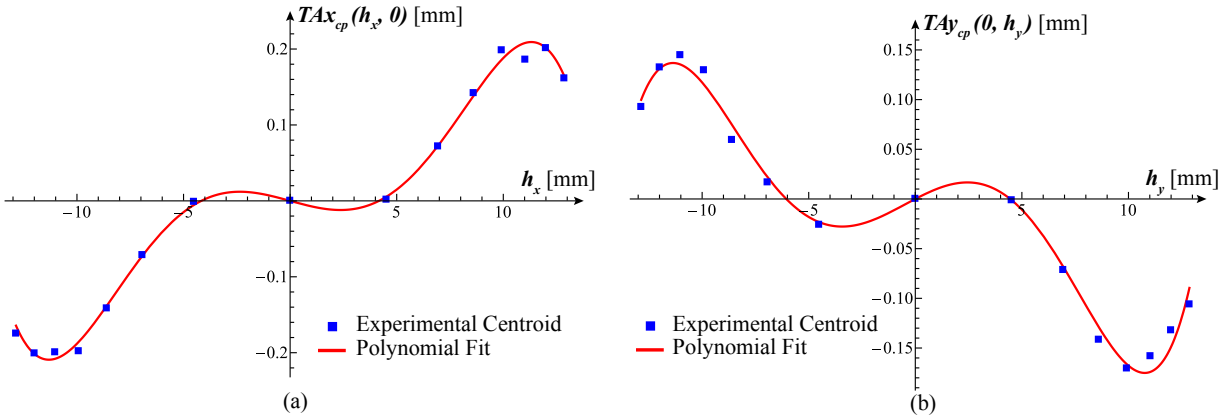

Figure 8. (a) Polynomial fit for transverse aberration TAx, for a group of sagittal centroids. (b) Polynomial fit transversal aberration TAy to a group of meridional centroids.

We make a polynomial fit for the convex-plane configuration, which is shown in Fig. 6, and is expressed as

$$\begin{aligned} ATx(h_x,0) = &\quad -0.00770643h_x + 0.000481314h_x^3 - 2.16128\times10^{-6}{h_x}^5, \\ ATy(0,h_y) = &\quad 0.0111625h_y - 0.000686222h_y^2 - 0.00047489h_y^3 \\ &+4.33676\times10^{-6}h_y^4 + 2.17417\times10^{-6}h_y^5, \end{aligned} \tag{7}$$

as we can see we have the influence of spherical aberration of fifth order. By using Eq.(6) we get the values for primary aberrations qualitatively as, $A_{cp} = 8.68202\times10^{-6}$, $B_{cp} = -16.50425\times10^{-6}$, $C_{cp} = -3.40361\times10^{-4}$, $D_{cp} = 6.18381\times10^{-4}$, $E_{cp} = 0$, and $A_5 = 2.17417\times10^{-6}$.

5. CONCLUSIONS

A simple method to design Null Screens type Hartmann by refraction through a plano-convex aspheric lens has been implemented by using an array of circular spots which were printed on acetate foil by using a laser printer at 1200dpi. This method opens the door to design null screens to test arbitrary lenses either outside or inside of the caustic region. The qualitative analysis of the centroids showed that this method is useful for evaluating the corresponding coefficients for primary aberrations.

Acknowledgments

This work has been partially supported by Programa de Apoyo a Proyectos de Investigación e Innovación Tecnológica – Universidad Nacional Autónoma de México (#*IT*101414 and # IN114414), Consejo Nacional de Ciencia y Tecnología (# 168570). The corresponding author is grateful to I. Goméz-García for valuable assistance and comments.

REFERENCES

1. Malacara D., [Optical Shop Testing], John Wiley & Sons, Inc., New Jersey, 361-397 (2007).
2. Salas-Peimbert D. P., *et. al.*, "Ophthalmic Lenses Measurement Using Hartmann Test," SPIE, **5622**, 102-106 (2004).
3. López-Ramírez J. M., Malacara-Doblado D., Malacara-Hernández D., "New Simple geometrical test for aspheric lenses and mirrors," Opt. Eng., **39**, 2143–2148 (2000).
4. Díaz-Uribe R., Campos-García M., "Null-screen testing of fast convex aspheric surfaces," Appl. Opt. **39**, 2670–2677 (2000).
5. Malacara D., Cornejo-Rodriguez A., "Null Ronchi test for aspherical surfaces," Appl. Opt., **8**, 1778–1780 (1974).
6. Cordero-Davila A., Cornejo-Rodriguez A., Cardona-Nunez O., "Null Hartmann and Ronchi-Hartmann test," Appl. Opt., **29**, 4618–4621 (1990).
7. Avendaño-Alejo M., Gonzalez-Utrera D., Qureshi N., Castañeda L., Ordóñez-Romero C. L., "Null Ronchi-Hartmann test for a lens," Opt. Exp. **18**, 21131–21137 (2010).
8. González-Utrera D., Avendaño-Alejo M., "Quantitative evaluation of a plano-convex parabolic lens," SPIE, **8011**, 80111G-1-7, (2011).
9. M. Avendaño-Alejo, D. González-Utrera and L. Castañeda, "Caustics in a meridional plane produced by plano-convex conic lenses," J. Opt. Soc. Am. A, **28**, 2619–2628 (2011).
10. Avendaño-Alejo M., "Caustics in a meridional plane produced by plano-convex aspheric lenses," J. Opt. Soc. Am. A, **30**, 501–508 (2013).
11. Castán-Ricaño D., Avendaño-Alejo M., "Designing null screens type sub-structured Ronchi to test a fast plano-convex aspheric lens," Proc. SPIE **9195**, 919509-1-7 (2014);
12. Rasban W., "ImageJ," Image Processing and Analysis in Java (National Institutes of Health), Vol. **1** 37, http://rsb.info.nih.gov/ij/.
13. Malacara D., Malacara Z., [Handbook of Lens Design], Marcel Dekker Inc., (1994).